Bioorganic & Medicinal Chemistry 17 (2009) 2744–2750

Contents lists available at ScienceDirect

Bioorganic & Medicinal Chemistry

journal homepage: www.elsevier.com/locate/bmc

Characteristic of neuraminidase inhibitory xanthones from *Cudrania tricuspidata*

Young Bae Ryu [a], Marcus J. Curtis-Long [c], Ji Won Lee [a], Jin Hyo Kim [a], Jun Young Kim [a], Kyu Young Kang [a], Woo Song Lee [b,*], Ki Hun Park [a,*]

[a] *Division of Applied Life Science (BK21 program), EB-NCRC, Institute of Agriculture and Life Science, Graduate School of Gyeongsang National University, Jinju 660-701, Republic of Korea*
[b] *Bioindustry Research Center, Korea Research Institute of Bioscience and Biotechnology (KRIBB), Jeongeup 580-185, Republic of Korea*
[c] *12 New Road, Nafferton, East Yorkshire YO25 4JP, UK*

ARTICLE INFO

Article history:
Received 14 January 2009
Revised 17 February 2009
Accepted 19 February 2009
Available online 26 February 2009

Keywords:
Cudrania tricuspidata
Xanthone
Neuraminidase
Time-dependent
2vk6

ABSTRACT

Natural polyphenolic compounds generally transpire to show relatively low inhibition against glycosidase including neuraminidase. In addition the inhibition modes of such compounds are rarely competitive. In this manuscript, a series of xanthone derivatives from *Cudrania tricuspidata* are shown to display nanomolar inhibitor activity against neuraminidase (EC 3.2.1.18) as well as competitive inhibition modes. Compound **8** bearing vicinal dihydroxy group on the A-ring displays nanomolar activity (IC_{50} = 0.08 ± 0.01 μM), a 200-fold increase in activity relative to that of the first reported xanthone-derived neuraminidase inhibitor, mangiferin (IC_{50} = 16.2 ± 4.2 μM). The 6,7-vicinal dihydroxy group plays a crucial role for inhibitory activity because compound **4**, which has one of these hydroxyl groups prenylated was inactive (33% at 200 μM), whereas other compounds (**1**–**3** and **6**–**8**) showed nanomolar activity (0.08–0.27 μM) and competitive inhibition modes. Interestingly all inhibitors manifested enzyme isomerization inhibition against neuraminidase. The most potent inhibitor, compound **8** showed similar interaction with a transition-state analogue of neuraminic acid in active site.

1. Introduction

Neuraminidase is a processing hydrolase involved in removing of terminal sialic acids from a variety of glycoconjugates.[1,2] It is known to play an important role in pathogenesis, bacterial nutrition, and cellular interaction. This enzyme specifically cleaves *N*-acetylneuraminic acid (NANA) from cell-surface glycoprotein when the sialic acid is joined to galactose via an α2→3 of α2→6 linkage.[3–5] Neuraminic acids (sialic acid) are generally found in the terminal position of the carbohydrate groups of glycolipids and glycoproteins. They have been proposed to play important roles in various biological processes by influencing the conformation of glycoproteins, recognizing and masking the biological sites of the molecules and their binding sites to cells.[6–8] Neuraminidase is especially believed to play at least two critical roles in influenza viral life cycle:[9–11] the facilitation of virion progeny release; and general mobility of the virus in the respiratory tract. Development of inhibitors of neuraminidase provides a new therapeutic approach for the treatment of the influenza virus and other diseases that arise from hydrolysis of sialic acid.[11] With the ever-present threat of a pandemic derived from the influenza virus, the importance of neuraminidase inhibitors escalates.[12]

There is considerable interest in the development of neuraminidase inhibitors from edible natural plants as these can be readily applied to neutraceutics for the prevention of virus infection: catechin derivatives are known to be strong inhibitors of the replication processes of both HIV[13] and the influenza virus,[14] in addition isoscutellarin-8-*O*-glucuronide from the leaf of *Scutellaria baicalensis* also possess potent mouse liver sialidase inhibition properties (IC_{50} = 40 μM).[15] When these and similar results are combined with data from cell-culture, it has been reported that flavonoids have a great potential to function as neuraminidase inhibitors.[15–17] Polyphenolic compounds are the most popular targets for neuraminidase, but so far their potency has been limited as IC_{50} values have been at best in the μM range.

Cudrania tricuspidata belongs to the Moraceae family and is widely distributed in Korea, China, and Japan. The roots of *C. tricuspidata* have been used for the treatment of gonorrhea, rheumatism, amenorrhea, bruising, and dysmenorrheal. Prenylated

Abbreviations: I, intensity at ex: 365 nm, em: 450 nm; IC_{50}, the inhibitor concentration leading to 50% activity loss; K_i, inhibition constant; K_i^{app}, apparent K_i; k_{obs}, apparent first-order rate constant for the transition from v_i to v_s; v_i, initial velocity; v_s, steady-state rate.

* Corresponding author. Tel.: +82 63 570 5170 (W.S.L.); tel.: +82 55 751 5472; fax: +82 55 757 0178 (K.H.P.).
E-mail addresses: wslee@kribb.re.kr (W.S. Lee), khpark@gsnu.ac.kr (K.H. Park).

0968-0896/$ - see front matter © 2009 Elsevier Ltd. All rights reserved.
doi:10.1016/j.bmc.2009.02.042

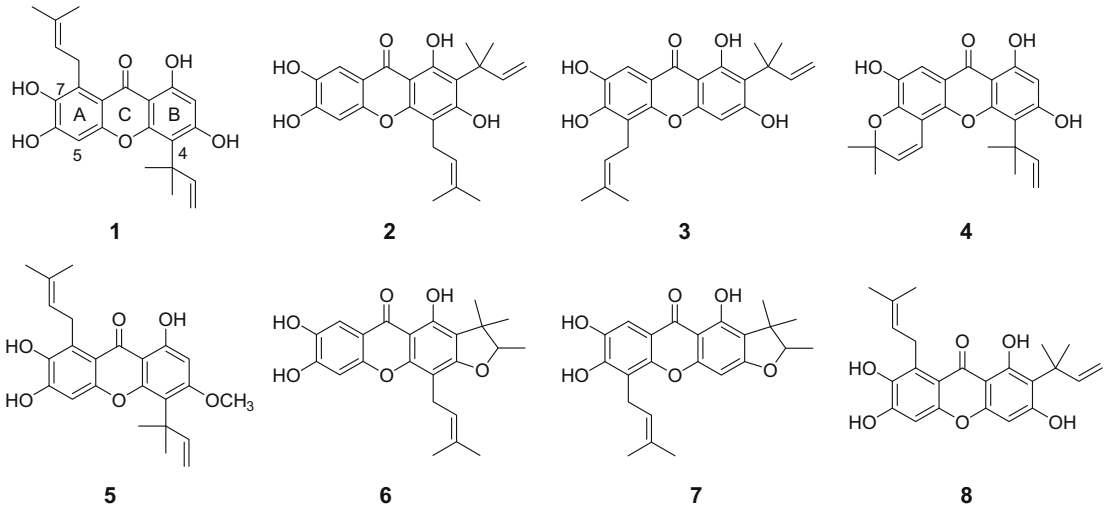

Figure 1. Chemical structures of isolated compounds **1**–**8** from the *Cudrania tricuspidata*.

xanthones and flavonoids are the major compound components of *C. tricuspidata*. Previous biological studies have shown that the constituents of *C. tricuspidata* exhibit anticancer[18] and antioxidant properties[18] as well as monoamine oxidase[19] (MAO) inhibitory activity. In our recent publications, we have begun to elucidate the vast biological potential of these extracts through various biological studies. For instance, xanthones possessing a vicinal dihydroxy group on one phenyl ring were shown to behave as excellent radical scavengers.[18] Xanthone-derived species were later proven to strongly suppress LDL oxidation.[20] We associated this with the anti-atherosclerotic and anti-inflammatory properties of *C. tricuspidata*. Our research has also brought to light that natural xanthones can inhibit α-glucosidase potently (at the low μM level).[21]

In this manuscript, we found that xanthones from *C. tricuspidata* inhibited neuraminidase at the nanomolar level. Moreover, these strongly potent inhibitors exhibited competitive inhibition, which is very rare in polyphenolic compounds. We also wish to report a detailed enzyme mechanism study and molecular docking experiments.

2. Results and discussion

2.1. Isolation and identification of xanthones derivatives

The EtOAc extract of the root of *C. tricuspidata* was selected for purification through activity (against neuraminidase)-guided fractionation. Repeated column chromatography of this extract furnished eight xanthones (**1**–**8**) (Fig. 1). The spectroscopic data of compounds (**1**–**8**) agree with those previously published[18,20,21] for Cudratricusxanthone (**1**), Macluraxanthone (**2**), Cudraxanthone L (**3**), 1,3,7-trihydroxy-4-(1,1-dimethyl-2-propenyl)-5,6-(2,2-dimethylchromeno) xanthone (**4**), Cudratricusxanthone F (**5**), Cudraxanthone D (**6**), Cudraxanthone M (**7**), and 1,3,6,7-tetrahydroxy-2-(3-methylbut-2-enyl)-8-(2-methylbut-3-en-2-yl)-9*H*-xanthen-9-one (**8**).

2.2. Effects of isolated xanthones on the activity of neuraminidase

In a preliminary screening using neuraminidase, we observed that EtOAc extracts of *C. tricuspidata* roots showed significant inhibition of the hydrolysis of neuraminic acid. In fractionation, guided by neuraminidase inhibitory activity, EtOAc fractions showed strong inhibitory activity against neuraminidase. More detailed bioassays of the isolated compounds (**1**–**8**) were subsequently conducted. As shown in Table 1, all 6,7-vicinal dihydroxy substituted xanthones (**1**–**8**) examined exhibited a dose-dependent inhibitory effect on the hydrolysis activity of neuraminidase (IC_{50} 0.08–1.27 μM) (Fig. 2A). These derivatives showed a 20-fold higher activity than quercetin and were 200 times more activate than the positive control, mangiferin (Table 1).[17,22] Compound **4** which bears a mono alkylated 6,7-dihydroxy motif was shown to have a much higher IC_{50} value (around 300 μM) (Table 1).

Raising the concentrations of the inhibitors drastically lowered residual enzyme activity (Fig. 2B). All inhibitors manifested a similar relationship between enzyme activity and enzyme concentration. The relevant data for compound **1** is illustrated in Figure 2B as an example. Plots of residual enzyme activity versus enzyme concentration at different concentrations of compound **1** gave a family of straight lines with a *y*-axis intercept of 0, indicating that **1** is a reversible inhibitor. Augmenting the concentration of compound **1** resulted in a reduction of the slopes of the lines.

2.3. Time-dependent inhibitory effects of xanthones on neuraminidase

To further investigate the inhibition mechanism, the time dependence of the inhibition of the hydrolysis of neuraminic acid by these inhibitors was subsequently probed. This was achieved

Table 1
Inhibitory effects of isolated compounds **1**–**8** on neuraminidase activities

Entry	IC_{50}[a] (μM)	Inhibition type (K_i, μM)
1	0.245 ± 0.03	Competitive (0.136 ± 0.01)
2	0.186 ± 0.02	Competitive (0.103 ± 0.02)
3	0.228 ± 0.01	Competitive (0.138 ± 0.02)
4	33% at 200 μM	Not tested
5	1.271 ± 0.21	Competitive (0.950 ± 0.02)
6	0.278 ± 0.08	Competitive (0.143 ± 0.02)
7	0.186 ± 0.04	Competitive (0.098 ± 0.01)
8	0.080 ± 0.01	Competitive (0.058 ± 0.01)
Quercetin[b]	2.7 ± 0.5	Not tested
Apigenin[b]	17.4 ± 0.7	Not tested
Mangiferin[b]	16.2 ± 4.24	Not tested

[a] All compounds were examined in a set of experiments repeated three times; IC_{50} values of compounds represent the concentration that caused 50% enzyme activity loss.
[b] These compounds were used as a positive control.

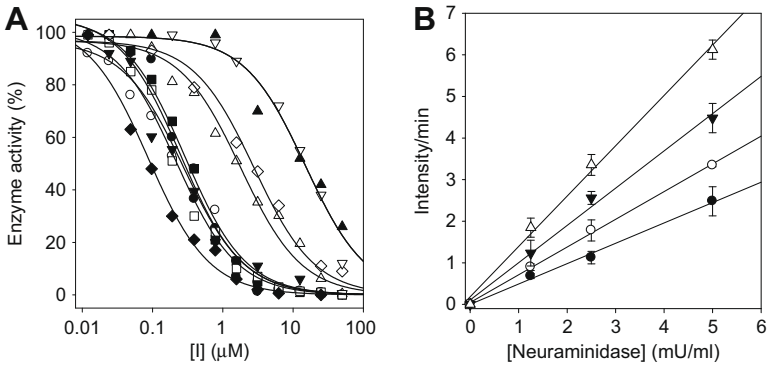

Figure 2. (A) Effects of compounds on the activity of neuraminidase for hydrolysis of neuraminic acid. (compound **1**, ●; compound **2**, ○; compound **3**, ▼; compound **5**, Δ; compound **6**, ■; compound **7**, □; compound **8**, ♦; quercetin, ◇; apigenin, ▲; mangiferin, ▽, respectively). (B) The hydrolytic activity of neuraminidase as function of enzyme concentrations at different concentrations of compound **1** (0, Δ; 80 nM, ▼; 160 nM, ○; 320 nM, ●, respectively).

Table 2
Kinetic parameters for time-dependent inhibitor of neuraminidase by compounds (**1**–**3** and **5**–**8**)

Entry	K_i^{app} (nM)[a]	k_5 (s^{-1})	k_6 (s^{-1})
1	213.5 ± 37.2	0.0093 ± 0.001	0.00015 ± 0.0001
2	477.2 ± 98.6	0.0066 ± 0.002	0.00029 ± 0.0001
3	567.6 ± 41.8	0.0092 ± 0.001	0.00044 ± 0.0002
5	2230 ± 300	0.0173 ± 0.004	0.00002 ± 0.0000
6	435.9 ± 11.2	0.0112 ± 0.005	0.00068 ± 0.0007
7	510.1 ± 27.2	0.0091 ± 0.001	0.00047 ± 0.0002
8	127.4 ± 10.7	0.0065 ± 0.001	0.00015 ± 0.0001

[a] All compounds were examined in a set of experiments repeated three times.

by measuring initial velocities of substrate hydrolysis as a function of preincubation time of the enzyme with the inhibitor. As a decrease in residual activity was seen as a function of preincubation time, compound **8** emerged to be a slow-binding inhibitor at low concentrations (Fig. 3A). Increasing preincubations time of compounds (**1**–**6** and **8**) led to a decrease in both the initial velocity (v_i) and the steady-state rate (v_s) (Fig. 3B). Representatively, Figure 3C showed typical progress curves for slow binding behavior, when the hydrolysis of substrate by neuraminidase in the presence of different compound **8** concentrations (0, 0.09, 0.19, 0.39, 0.78, 1.56, and 3.12 μM). As shown in Figure 3C and D, the progress curves obtained using the differing concentrations of the inhibitors were fitted to Eq. 3 to determine k_{obs}. The plot presents the relationship between k_{obs} and concentrations of inhibitors [I]. The y intercept of the curve provides an estimate of the rate constant k_6, while the maximum value of k_{obs} expected at infinite inhibitor concentration. The kinetic parameters k_5, k_6, and K_i^{app}, were derived from the plots by fitting the results (Table 2). This, analysis unearthed the following values: $k_5 = 0.0065\ s^{-1}$, $k_6 = 0.00015\ s^{-1}$, and $K_i^{app} = 127.4$ nM. The kinetic model can be written as:[23]

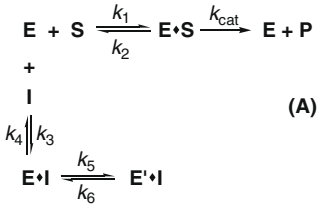

The plot showed a hyperbolic dependence on the concentration of the compound **8**, so the inhibition of neuraminidase by compound **8** is believed to followed mechanism A. The results indicated that **8** inhibits neuraminidase by rapid formation of an enzyme substrate complex (E·I) which slowly isomerizes to form a modified enzyme complex (E′·I).

2.4. Determination of the inhibition type of xanthones on neuraminidase

The inhibition mechanisms displayed by isolated xanthones (**1**–**3** and **5**–**8**) were then studied. This began with analysis of the mode of inhibition using both Lineweaver–Burk (Fig. 4A–F) and Dixon plot which is useful in determining the K_i value for inhibitor (Fig. 4G and H). As illustrated in Figure 4, the kinetic plots show that compounds (**1**–**3** and **5**–**8**) have respective inhibition constants, K_i of 0.136, 0.103, 0.138, 0.950, 0.143, 0.098, and 0.058 μM (Table 1). This analysis also delineates that the inhibitors are competitive because increasing concentration of substrate resulted in a family lines which declined with a common intercept on the x-axis ($-K_i$).

The predominant inhibition mode shown by naturally occurring neuraminidase inhibitors is noncompetitive. Interestingly, the inhibition of other enzymes by xanthone derives from *C. tricuspidata* is also rarely competitive. However, the xanthones in this manuscript showed time-dependent competitive inhibition of neuraminidase (enzyme isomerization inhibition). Thus these inhibitors may be correlated to Tamiflu® which inhibits neuraminidase from influenza virus A (Tokyo/3/67, N2) is a similar manner.[24] This suggests that further research on these important lead compounds may possibly show them to be alternative new anti-influenza treatments.

The qualitative SAR of these compounds can be described as follows. A vicinal dihydroxy motif on the A ring is mandatory for high activity, as compound **4**, in which one of the alcohol functions within this unit is blocked, showed at least 500 times less activity than **1**–**3** and **5**–**8** all of which have a free vicinal dihydroxy group in the ring A. Interestingly, blocking of one of the hydroxyl units of the 1,3-diol in the B ring appears to exert a variable but not insignificant effect on activity. Thus compounds **5**, **6**, and **7** all of which are alkylated at C3OH (on the B ring) have IC_{50} values 1.271 μM, 0.278 μM, and 0.186 μM, respectively, making them some of the least active species tested. When these are compared to the corresponding compounds bearing a free OH at C3, (**1**, **2**, and **3**) the IC_{50}s of the latter are generally (but not in the case of **3** vs **7**) lower. This outlines a moderately importantly role for the 1,3-diol unit in the B ring, which is presumably modified by other factors. The affects of alkyl substitution around the ring seem to be suitable and within experimental error are difficult to interpret.

2.5. *In silico* molecular docking simulation of xanthones

The excellent results outlined above spurred us on to investigate the principal interactions between the inhibitor and enzyme

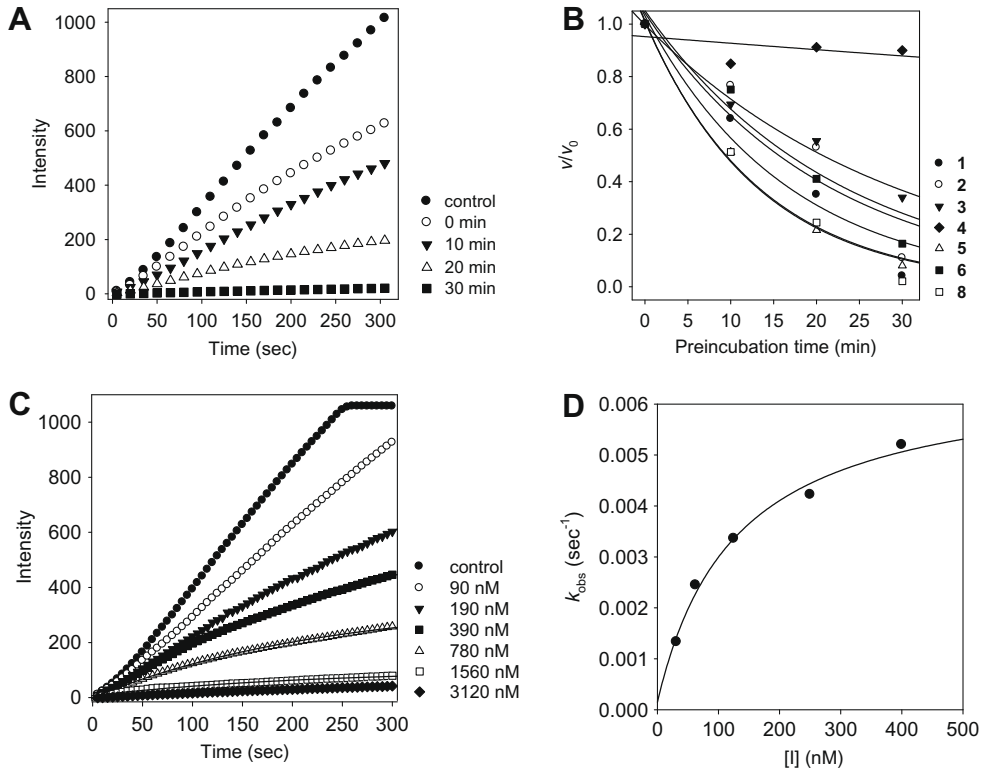

Figure 3. (A) Time-dependent inhibition of neuraminidase in the presence of **8** (at 80 nM). (B) Inhibition as a function of preincubation time for active compounds (**1**–**6** and **8**) at IC_{50}. (C) Slow-binding inhibition of compound **8** at time course. The k_{obs} values at each inhibition concentration were determined by fitting the data to Eq. 2. (D) Dependence of the values for k_{obs} on the concentration of compound **8**. The k_{obs} values, determined in panel A, were fitted to Eq. 3.

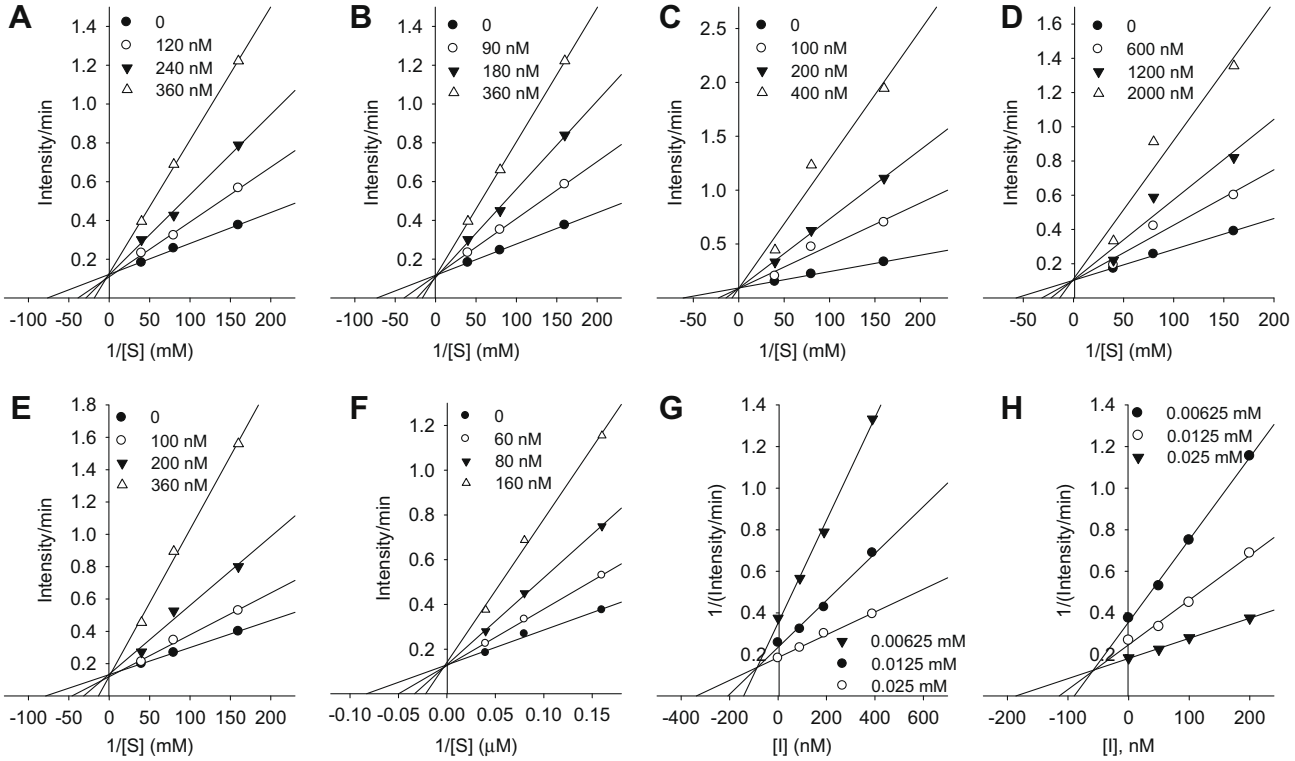

Figure 4. Graphical determination of the type of inhibition for compounds (**1**–**3**, **5**, **7**, and **8**). (A–F) Lineweaver–Burk plot for inhibition of compounds (**1**–**3**, **5**, **7**, and **8**) on neuraminidase for the hydrolysis of substrate. (G and H) Dixon plot for inhibition of compounds **1** and **8** on neuraminiase for the hydrolysis of substrate.

more thoroughly. The most potent inhibitor of neuraminidase, compound **8**, was analyzed via molecular docking analysis for its interactions with protein residues in the original ligand site. The X-ray structure of neuraminidase determined by Newstead[25] was obtained from the protein data bank (PDB Code 2vk6). Molecular docking studies were carried our using CDOCKER methodology[26] because of our kinetic study showing competitive inhibition mode. Figure 5A shows an overlay of the active site of the ligand free structure and compound **8**. Our modeling calculation unveiled H-bond interaction in the original ligand site between **8** and: Arg1266, Arg1285, Arg1555, and Asp1328 (Fig 5B). Interestingly, the binding pocket matches compound **8** very well. Furthermore this interaction appears to be similar to the interaction between the enzyme and 2-deoxy-2,3-dehydro-*N*-acetyl neuraminic acid (Neu5Ac2en) (Fig 5D inset)[25] which is a transition-state analogue of neuraminic acid as shown in Figure 5C and D. By comparing the interactions of these two ligands with Asp1328 and Arg1266, it seems likely that the 6,7-dihydroxy group of A-ring may bind to the protein in a similar fashion to the 4-OH and 5-NHAc of Neu5Ac2en, while the 7-OH of the xanthone assumes the role of 5-NHAc on Neu5Ac2en. In addition the carbonyl group of xanthone **8** may serve as a similar donor to the carboxylic acid moiety of Neu5Ac2en, both of which were found to interact with Arg1555. This result furnishes some additional support to our affirmation that xanthone **8** is a new lead competitive inhibitor for neuraminidase. Although this preliminary molecular modeling study cannot constitute a definitive proof for our argument, it is a positive sign that our inhibitor resides in the active site, as a competitive inhibitor should. It is also encouraging that taken as a whole the conclusion from modeling and SAR are in agreement.

3. Conclusion

Eight polyhydroxylated xanthones from *C. tricuspidiata* were isolated and shown to be particularly effective inhibitors of neuraminidase. Our detailed kinetic analysis of these species has unveiled that they are all competitive, slow binding inhibitors. Such characteristics are highly unusual for xanthones obtained from natural sources. We proceeded to investigate the interaction of these compounds with the enzyme by molecular modeling, which disclosed important information about the principal interactions bringing about activity in this series. Most importantly, the most active inhibitor, **8**, appeared to interact with the enzyme in a similar fashion to a known transition-state analogue. We strongly believe that all this information implicates xanthones **1**–**8** as potentially fruitful areas for antiviral drugs of the future.

4. Materials and methods

4.1. General apparatus and chemicals

All the reagent grade chemicals were purchased from Sigma Chemical Co. (St. Louis, MO, USA). Chromatographic separations were carried out by Thin–layer Chromatography (TLC) (E. Merck Co., Darmastdt, Germany), using commercially available glass plate pre–coated with silica gel and visualized under UV at 254 and 366 nm sprayed with *p*-anisaldehyde staining reagent. Column chromatography was carried out using 230–400 mesh Silica Gel (kieselgel 60, Merck, Germany). Silica gel (230–400 mesh, Merck), RP-18 (ODS-A, 12 nm, S-150 mM, YMC), and Sephadex LH-20 (Amersham Biosciences) were used for column chromatography. Melting points were measured on a Thomas Scientific Capillary Melting Point Apparatus and are uncorrected. IR spectra were recorded on a Bruker IFS66 infrared Fourier transform spectrophotometer (KBr). ^{1}H and ^{13}C NMR along with 2D-NMR data were obtained on a Bruker AM 500 (^{1}H NMR at 500 MHz, ^{13}C NMR at 125 MHz) spectrometer in $CDCl_3$ acetone-d_6, DMSO-d_6, and CD_3OD, EIMS and HREIMS data were collected on Jeol JMS-700 spectrometer. Optical rotations were measured on Perkin–Elmer 343 polarimeter.

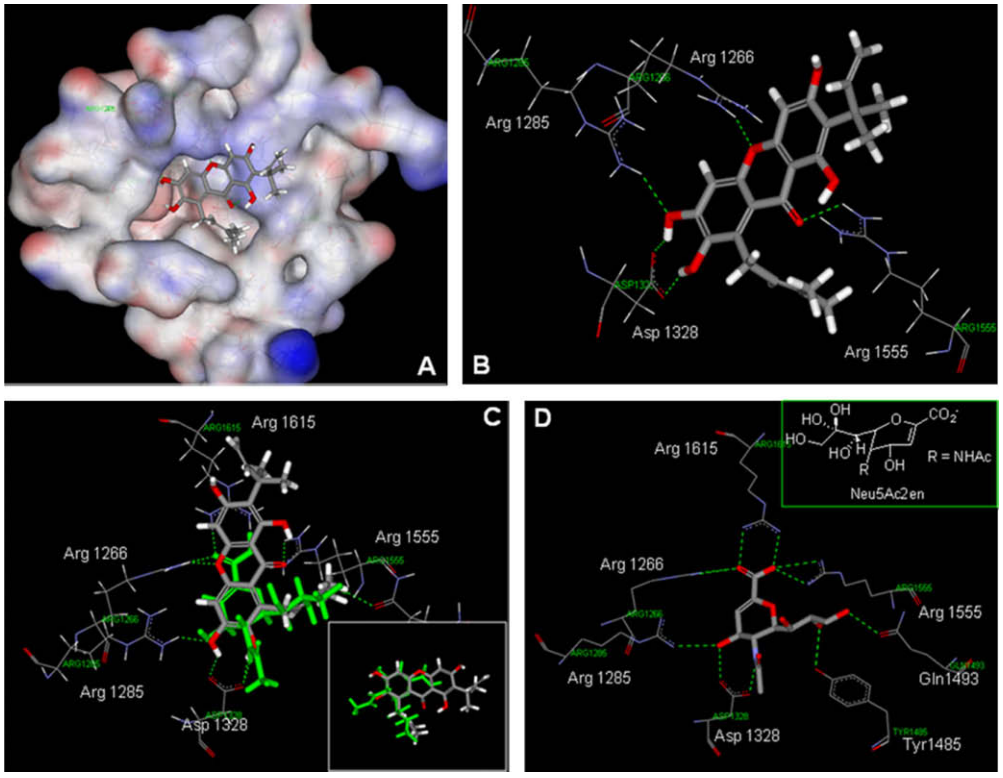

Figure 5. (A) Overlay of the active site of the ligand free structure and compound **8**. (B) Hydrogen bond interactions between compound **8** and neuraminidase. (C and D) Compound **8** binding pocket matches with Neu5Ac2en on the structure at active site of neuraminidase (green color, Neu5Ac2en).

4.2. Isolation of neuraminidase inhibitors from *C. tricuspidata*

The root bark of *C tricuspidata* (Carr.) Bureau was collected in Hapchun (Korea) in August, 2002, and identified by Professor Jae-Hong Pak of Kyungpook National University. A voucher specimen (Park, K. H. 110) of this raw material is deposited at the Herbarium of Kyungpook National University (KNU). The root bark of *C. tricuspidata* (2 kg) were air-dried, pulverized, and extracted with EtOAc for a week at room temperature. The combined extract was evaporated to dryness under reduced pressure at a temperature below 35 °C to afford EtOAc-soluble extracts (61 g). The EtOAc extract was subjected to column chromatography on silica gel (10 × 30 cm, 230–400 mesh, 600 g) using hexane/EtOAc [40:1 (1.5 L), 20:1 (1.5 L), 10:1 (1.5 L), 5:1 (1.5 L), 3:1 (1.5 L), 1:1 (3 L) and only EtOAc (3 L)] mixtures to give fractions F1–F5. Fraction F3 (18 g) was purified by column chromatography using a glass column packed with silica gel in hexane/EtOAc. The column was then eluted using hexane/acetone (40:1→1:1) mixtures of increasing polarity. Altogether, 80 fractions of 100 mL each were collected and combined to give seven major subfractions (F3.1–F3.7), based on the comparison of TLC profile using hexane/acetone (3:1) as developing solvent. Subfraction F3.1 (1.8 g) was rechromatographed using the same solvent gradient, to yields compound **3** (12 mg) and compound **4** (33 mg). Subfraction F3.3 (1.2 g) were purified using sephadex LH-20 column chromatography, eluting with 95% MeOH to afford compound **1** (30 mg), compound **2** (22 mg), and compound **5** (14 mg). Furthermore, compounds **1**–**3** were purified by recrystallized from hexane/acetone. Subfraction F3.6 (2.2 g) was subjected to silica gel column (3 × 50 cm, 230–400 mesh, 250 g) chromatography with hexane/EtOAc (40:1→1:1) and then purified by reversed-phase column chromatography. Thus, this subfraction was loaded onto a glass column packed with RP-18 (ODS-A, 12 nm, S-150 μM, 40 g). The column was then eluted using MeOH/H_2O (4:1) to afford compound **8** (8 mg). Fraction 4 (10 g) was applied to silica gel column [eluent: hexane/EtOAc (40:1→1:1)] to afford 12 fractions (F4.1–F4.12). Subfraction F4.7 (750 mg) was resubjected to silica gel chromatography with hexane/acetone (30:1→1:1) to yield compound **6** (11 mg) and **7** (9 mg). All of isolated compounds were identified on the basis of the following spectroscopic data.

Compound **1** obtained as a yellowish solid; ^{1}H NMR (500 MHz, $CDCl_3$) δ 6.22 (1H, s, H-2), 6.79 (1H, s, H-5), 1.68 (3H, s, H-12), 1.68 (3H, s, H-13), 6.45 (1H, dd, J = 17.8, 10.5 Hz, H-14), 5.35 (1H, d, J = 10.5 Hz, H-15), 5.44 (1H, d, J = 17.8 Hz, H-15), 4.27 (2H, d, J = 6.7 Hz, H-16), 5.30 (1H, m, H-17), 1.75 (3H, s, H-19), 1.87 (3H, s, H-20). ^{13}C NMR (125 MHz, $CDCl_3$) δ 161.7 (C-1), 100.0 (C-2), 161.8 (C-3), 108.9 (C-4), 155.0 (C-4a), 152.9 (C-4b), 100.6 (C-5), 150.9 (C-6), 140.0 (C-7), 127.4 (C-8), 111.1 (C-8a), 183.0 (C-9), 104.6 (C-9a), 40.8 (C-11), 28.1 (C-12), 28.1 (C-13), 149.4 (C-14), 113.1 (C-15), 26.0 (C-16), 121.6 (C-17), 135.0 (C-18), 18.1 (C-19), 25.9 (C-20).[18,20,21]

Compound **2** obtained as a yellowish prism; ^{1}H NMR (500 MHz, $CDCl_3$) δ 6.41 (1H, s, H-5), 7.51 (1H, s, H-8), 1.68 (3H, s, H-12), 1.68 (3H, s, H-13), 6.53 (1H, dd, J = 17.8, 10.5 Hz, H-14), 5.40 (1H, d, J = 10.5 Hz, H-15), 5.30 (1H, d, J = 17.8 Hz, H-15), 3.44 (2H, d, J = 7.0 Hz, H-16), 5.20 (1H, m, H-17), 1.70 (3H, s, H-19), 1.83 (3H, s, H-20). ^{13}C NMR (125 MHz, $CDCl_3$) δ 160.4 (C-1), 113.2 (C-2), 161.1 (C-3), 107.2 (C-4), 153.3 (C-4a), 151.8 (C-4b), 102.1 (C-5), 152.8 (C-6), 141.9 (C-7), 107.0 (C-8), 112.1 (C-8a), 180.3 (C-9), 102.6 (C-9a), 41.5 (C-11), 27.4 (C-12), 27.4 (C-13), 149.9 (C-14), 113.4 (C-15), 22.1 (C-16), 122.3 (C-17), 131.8 (C-18), 17.9 (C-19), 25.8 (C-20).[18,20,21]

Compound **3** obtained as a yellowish needle; ^{1}H NMR (500 MHz, CD_3OD) δ 6.32 (1H, s, H-4), 7.35 (1H, s, H-8), 1.61 (3H, s, H-12), 1.61 (3H, s, H-13), 6.35 (1H, dd, J = 17.8, 10.6 Hz, H-14), 4.81 (1H, d, J = 10.6 Hz, H-15), 4.90 (1H, d, J = 17.5 Hz, H-15), 3.51 (2H, d, J = 7.1 Hz, H-16), 5.23 (1H, m, H-17), 1.65 (3H, s, H-19), 1.85 (3H, s, H-20). ^{13}C NMR (125 MHz, CD_3OD) δ 163.7 (C-1), 116.3 (C-2), 165.7 (C-3), 95.5 (C-4), 157.6 (C-4a), 151.3 (C-4b), 116.3 (C-5), 152.9 (C-6), 144.2 (C-7), 106.7 (C-8), 114.0 (C-8a), 182.1 (C-9), 103.7 (C-9a), 42.5 (C-11), 29.9 (C-12), 29.9 (C-13), 152.0 (C-14), 108.5 (C-15), 23.7 (C-16), 123.3 (C-17), 133.1 (C-18), 18.6 (C-19), 26.4 (C-20).[18,20,21]

Compound **4** obtained as a yellowish powder; ^{1}H NMR (500 MHz, $CDCl_3$) δ 6.15 (1H, s, H-2), 6.77 (1H, s, H-8), 1.43 (3H, s, H-12), 1.43 (3H, s, H-13), 6.39 (1H, dd, J = 17.8, 10.5 Hz, H-14), 5.41 (1H, d, J = 10.5 Hz, H-15), 5.39 (1H, d, J = 17.8 Hz, H-15), 7.93 (2H, d, J = 10.2 Hz, H-16), 5.75 (1H, d, J = 10.2 Hz, H-17), 1.62 (3H, s, H-19), 1.63 (3H, s, H-20). ^{13}C NMR (125 MHz, $CDCl_3$) δ 162.2 (C-1), 100.6 (C-2), 162.4 (C-3), 109.4 (C-4), 155.6 (C-4a), 137.4 (C-4b), 120.0 (C-5), 151.4 (C-6), 153.0 (C-7), 102.3 (C-8), 108.5 (C-8a), 183.2 (C-9), 105.0 (C-9a), 41.3 (C-11), 28.4 (C-12), 28.4 (C-13), 149.7 (C-14), 113.7 (C-15), 121.3 (C-16), 132.8 (C-17), 77.5 (C-18), 27.7 (C-19), 27.7 (C-20).[18,20,21]

Compound **5** obtained as a yellowish needle; ^{1}H NMR (500 MHz, $CDCl_3$) δ 6.32 (1H, s, H-2), 6.80 (1H, s, H-5), 1.62 (3H, s, H-12), 1.62 (3H, s, H-13), 6.25 (1H, dd, J = 17.4, 10.6 Hz, H-14), 4.84 (1H, d, J = 10.6 Hz, H-15), 4.85 (1H, d, J = 17.4 Hz, H-15), 4.30 (2H, d, J = 6.8 Hz, H-16), 5.30 (1H, m, H-17), 1.77 (3H, s, H-19), 1.88 (3H, s, H-20), 3.82 (OCH_3). ^{13}C NMR (125 MHz, $CDCl_3$) δ 162.4 (C-1), 95.6 (C-2), 165.1 (C-3), 112.7 (C-4), 154.7 (C-4a), 153.8 (C-4b), 101.3 (C-5), 151.4 (C-6), 140.0 (C-7), 127.6 (C-8), 111.3 (C-8a), 183.6 (C-9), 104.5 (C-9a), 41.5 (C-11), 29.8 (C-12), 30.1 (C-13), 151.2 (C-14), 107.3 (C-15), 26.4 (C-16), 121.9 (C-17), 135.9 (C-18), 26.2 (C-19), 18.5 (C-20), 55.9 (OCH_3).[18,20,21]

Compound **6** obtained as a pale yellow; ^{1}H NMR (500 MHz, acetone-d_6) δ 6.84 (1H, s, H-5), 7.41 (1H, s, H-8), 1.35 (3H, s, H-12), 1.11 (3H, s, H-13), 4.39 (1H, q, J = 13.1, 6.6 Hz, H-14), 1.26 (3H, d, J = 6.6 Hz, H-15), 3.26 (2H, d, J = 7.2 Hz, H-16), 5.27 (1H, br t, J = 7.2 Hz, H-17), 1.72 (3H, s, H-19), 1.52 (3H, s, H-20). ^{13}C NMR (125 MHz, acetone-d_6) δ 157.7 (C-1), 117.0 (C-2), 164.6 (C-3), 103.2 (C-4), 156.1 (C-4a), 153.0 (C-4b), 103.9 (C-5), 154.5 (C-6), 144.5 (C-7), 109.6 (C-8), 114.0 (C-8a), 181.6 (C-9), 104.6 (C-9a), 44.8 (C-11), 21.4 (C-12), 26.0 (C-13), 91.7 (C-14), 15.1 (C-15), 23.0 (C-16), 123.3 (C-17), 132.5 (C-18), 18.4 (C-19), 26.3 (C-20).[18,20,21]

Compound **7** obtained as a yellowish powder; ^{1}H NMR (500 MHz, $CDCl_3$) δ 6.33 (1H, s, H-4), 7.50 (1H, s, H-8), 1.26 (3H, s, H-12), 1.51 (3H, s, H-13), 4.54 (1H, q, J = 6.6 Hz, H-14), 1.42 (3H, d, J = 6.6 Hz, H-15), 3.25 (2H, m, H-16), 5.14 (1H, m, H-17), 1.81 (3H, s, H-19), 1.65 (3H, s, H-20). ^{13}C NMR (125 MHz, $CDCl_3$) δ 158.1 (C-1), 116.7 (C-2), 165.8 (C-3), 89.3 (C-4), 158.0 (C-4a), 150.0 (C-4b), 115.1 (C-5), 149.9 (C-6), 141.6 (C-7), 105.1 (C-8), 112.4 (C-8a), 180.3 (C-9), 103.4 (C-9a), 43.4 (C-11), 20.7 (C-12), 25.2 (C-13), 91.1 (C-14), 14.4 (C-15), 22.2 (C-16), 121.0 (C-17), 132.8 (C-18), 17.9 (C-19), 25.7 (C-20).[18,20,21]

Compound **8** obtained as a yellowish solid; ^{1}H NMR (500 MHz, $CDCl_3$) δ 7.43 (1H, s, H-4), 6.29 (1H, s, H-5), 1.59 (3H, s, H-12), 1.59 (3H, s, H-13), 6.46 (1H, dd, J = 17.8, 10.6 Hz, H-14), 5.34 (1H, d, J = 10.6 Hz, H-15a), 5.34 (1H, d, J = 17.8 Hz, H-15b), 3.09 (2H, d, J = 7.0 Hz, H-16), 5.01 (1H, d, J = 7.0 Hz, H-17), 1.56 (3H, s, H-19), 1.72 (3H, s, H-20). ^{13}C NMR (125 MHz, $CDCl_3$) δ 163.0 (C-1), 113.6 (C-2), 163.3 (C-3), 95.8.9 (C-4), 156.4 (C-4a), 142.0 (C-4b), 105.4 (C-5), 150.7 (C-6), 150.1 (C-7), 115.6 (C-8), 112.6 (C-8a), 180.8 (C-9), 103.1 (C-9a), 41.5 (C-11), 27.5 (C-12), 27.4 (C-13), 150.2 (C-14), 113.9 (C-15), 22.3 (C-16), 121.3 (C-17), 133.2 (C-18), 26.1 (C-19), 18.3 (C-20).[21]

4.3. Assay of neuraminidase activity

Neuraminidase activity was measured by a modification of the method described by Poteir et al.[17,27] 4-Methylumbelliferyl-α-D-*N*-

acetylneuraminic acid sodium salt hydrate (SIGMA, M8639) 0.125 mM in 50 mM sodium acetate buffer (pH 5.0) was used as a substrate. Neuraminidase (E.C. 3.2.1.18. from *Clostridium perfringens*, SIGMA, N2876) 0.1 U/mL in acetate buffer was used as the enzyme. The isolated compounds were dissolved in MeOH and diluted to the corresponding concentrations in acetate buffer. For assay, enzyme (15 μL) was added to 15 μL of sample solution mixed with buffer (510 μL) in a cuvette, and then was added 60 μL of substrate at 37 °C. 4-Methylumbelliferone was immediately quantified by fluorometric determination with an LS-55 luminescence spectrometer (Perkin–Elmer Limited, Beaconsfield, Buckinghamshire, United Kingdom). The excitation wavelength was 365 nm, with the excitation slits set at 2.5 nm, and the emission wavelength was 450 nm, with the emission slits set at 20 nm. For the determination of enzyme activity (by fitting experimental data to the logistic curve by Eq. 1), used time-drive protocol with initial velocity was recorded over a range of concentrations and the data were analyzed using a nonlinear regression program [Sigma Plot (SPCC Inc., Chicago, IL)].

$$\text{Activity } (\%) = 100[1/(1 + ([\text{I}]/\text{IC}_{50}))] \quad (1)$$

4.4. Progress curves determination and time-dependent assay

Time-dependent assays and progress curves were carried out using 0.1 U/mL units neuraminidase, and 4-methylumbelliferyl-α-D-*N*-acetylneuraminic acid sodium salt hydrate (SIGMA, M8639) as a substrates in 0.05 M sodium acetate buffer (pH 5.0) at 37 °C. Enzyme activities were measured by fluorimetry continuously for 5 min. To determine the kinetic parameters associated with time-dependent inhibition of neuraminidase, progress curves for 300 s were obtained at several inhibitor concentrations using fixed substrate concentrations. The data were analyzed using the a nonlinear regression program [Sigma Plot (SPCC Inc., Chicago, IL)] to give the individual parameters for each curve; v_i (initial velocity), v_s (steady-state velocity), k_{obs} (apparent first-order rate constant for the transition from v_i to v_s), I (intensity at ex: 365 nm, em: 450 nm), and K_i^{app} (apparent K_i) according to the following equations:[23]

$$I = v_s t + (v_i - v_s)[1 - \exp(-k_{obs} t)]/k_{obs} \quad (2)$$

$$k_{obs} = k_6 + [(k_5 \times [\text{I}])/(K_i^{app} + [\text{I}])] \quad (3)$$

4.5. Simulation of molecular docking

The neuraminidase three-dimensional structures were obtained from Protein Data Bank (PDB), accession code no. was 2vk6.[25] CDOCKER protocol in Discovery Studio platform was used for the docking studies. After water molecules and inhibitor were removed from 2vk6 (whole structure), the crystal structure was defined as the receptor and the active site was defined as a sphere within 8 Å reach of the inhibitor. Random ligand conformations are generated from the initial ligand structure through high temperature molecular dynamics, followed by random rotations.[26]

Acknowledgments

This work was supported by a grant from Agricultural R&D Promotion Center, Korea Rural Economic Institute and the MOST/KOSEF to the EB-NCRC (R15-2003-012-0200-0), Republic of Korea. J.W.L. was supported by a scholarship from the BK21 Program, the Ministry of Education and Human Resources Development, Republic of Korea.

Supplementary data

Supplementary data associated with this article can be found, in the online version, at doi:10.1016/j.bmc.2009.02.042.

References and notes

1. Schauer, R.; Kelm, S.; Reuter, G.; Roggenin, P. In *Biology of the Sialic Acid*; Rosenberg, A., Ed.; Plenum Press: New York, 1995; pp 7–67.
2. Saito, M.; Yu, R. K. In *Biology of the Sialic Acid*; Rosenberg, A., Ed.; Plenum Press: New York, 1995; pp 216–313.
3. Matrosovich, M. N.; Matrosovich, T. Y.; Gray, T.; Roberts, N. A.; Klenk, H. D. *Proc. Natl. Acad. Sci. U.S.A.* **2004**, *101*, 4620.
4. Shinya, K.; Ebina, M.; Yamada, S.; Ono, M.; Kasai, N.; Kawaoka, Y. *Nature* **2006**, *440*, 435.
5. Couceiro, J. N.; Paulson, J. C.; Baum, L. G. *Virus Res.* **1993**, *29*, 155.
6. Monti, E.; Preti, A.; Venerando, B.; Borsani, G. *Neurochem. Res.* **2002**, *27*, 649.
7. Achyuthan, K. E.; Achyuthan, A. M. *Comp. Biochem. Physiol. B: Biochem. Mol. Biol.* **2001**, *129*, 29.
8. Rosenberg, A.; Schengrund, C.-L. In *Biological Roles of Sialic Acid*; Rosenberg, A., Ed.; Plenum: New York, 1976; pp 295–359.
9. Garman, E.; Laver, G. *Protein Rev.* **2005**, *1*, 247.
10. Ohuchi, M.; Asaoka, N.; Sakai, T.; Ohuchi, R. *Microbes Infect.* **2006**, *8*, 1287.
11. Skehel, J. J.; Wiley, D. C. *Annu. Rev. Biochem.* **2000**, *69*, 531.
12. Garman, E.; Laver, G. *Curr. Drug Targets* **2004**, *5*, 119.
13. (a) Fassina, G.; Buffa, A.; Benelli, R.; Varnier, O. E.; Noonanm, S. K.; Li, C.; Liu, S. T. *Biochem. Biophys. Res. Commum.* **2002**, *16*, 939; (b) Nakane, H.; Ono, K. *Biochemistry* **1990**, *29*, 2841.
14. (a) Song, J.-M.; Lee, K.-H.; Seong, B.-L. *Antiviral Res.* **2005**, *68*, 66; (b) Song, J. M.; Park, K. D.; Lee, K. H.; Byun, Y. H.; Park, J. H.; Kim, S. H.; Kim, J. H.; Seong, B. L. *Antiviral Res.* **2007**, *76*, 178.
15. Nagai, T.; Miyaichi, Y.; Tomimori, T.; Yamada, H. *Biochem. Biophys. Res. Commun.* **1989**, *163*, 25.
16. Nagai, T.; Miyaichi, Y.; Tomimori, T.; Yamada, H. *Chem. Pharm. Bull.* **1990**, *38*, 1329.
17. Ryu, Y. B.; Curtis-Long, M. J.; Kim, J. H.; Jeong, S. H.; Yang, M. S.; Lee, K. W.; Lee, W. S.; Park, K. H. *Bioorg. Med. Chem. Lett.* **2008**, *18*, 6046.
18. (a) Lee, B. W.; Lee, J. H.; Lee, S. T.; Lee, H. S.; Lee, W. S.; Jeong, T. S.; Park, K. H. *Bioorg. Med. Chem. Lett.* **2005**, *15*, 5548; (b) Lee, B. W.; Gal, S. W.; Park, K. M.; Park, K. H. *J. Nat. Prod.* **2005**, *68*, 456.
19. Han, X. H.; Hong, S. S.; Hwang, J. S.; Jeong, S. H.; Hwang, J. H.; Lee, M. H.; Lee, M. K.; Lee, D.; Ro, J. S.; Hwang, B. Y. *Arch. Pharm. Res.* **2005**, *28*, 1324.
20. Park, K. H.; Park, Y. D.; Han, J. M.; Im, K. R.; Lee, B. W.; Jeong, I.-Y.; Jeong, T. S.; Lee, W. S. *Bioorg. Med. Chem. Lett.* **2006**, *16*, 5580.
21. Seo, E. J.; Curtis-Long, M. J.; Lee, B. W.; Kim, H. Y.; Ryu, Y. B.; Jeong, T.-S.; Lee, W. S.; Park, K. H. *Bioorg. Med. Chem. Lett.* **2007**, *17*, 6421.
22. Li, X.; Ohtsuki, T.; Shindo, S.; Sato, M.; Koyano, T.; Preeprame, S.; Kowithayakorn, T.; Ishibashi, M. *Planta Med.* **2007**, *73*, 1195.
23. Morrison, J. F.; Walsh, C. T. *Adv. Enzymol.* **1988**, *61*, 201.
24. Kati, W. M.; Saldivar, A. S.; Mohamadi, F.; Sham, H. L.; Laver, W. G.; Kohlvrenner, W. E. *Biochem. Biophys. Res. Commun.* **1998**, *244*, 408.
25. Newstead, S. L.; Potter, J. A.; Wilson, J. C.; Xu, G.; Chien, C.-H.; Watts, A. G.; Withers, S. G.; Taylor, G. L. *J. Biol. Chem.* **2008**, *283*, 9080.
26. Wu, G.; Robertson, D. H.; Brooks, C. L., III; Vieth, M. *J. Comput. Chem.* **2003**, *24*, 1549.
27. Potier, M.; Mameli, L.; Belisle, M.; Dallaire, L.; Melancon, S. B. *Anal. Biochem.* **1979**, *94*, 287.